Almost Enclosed Buckyball Joints: Synthesis, Complex Formation, and Computational Simulations of Pentypticene-Extended Tribenzotriquinacene

Stefan Henne,[a] Björn Bredenkötter,[a] Mohammad Alaghemandi,[b] Sareeya Bureekaew,[b] Rochus Schmid,*[b] and Dirk Volkmer*[a]

We report the synthesis of a tribenzotriquinacene-based (TBTQ) receptor (**3**) for C_{60} fullerene, which is extended by pentiptycene moieties to provide an almost enclosed concave ball bearing. The system serves as a model for a self-assembling molecular rotor with a flexible and adapting stator. Unexpectedly, nuclear magnetic resonance spectroscopic investigations reveal a surprisingly low complex stability constant of $K_1 = 213 \pm 37\ M^{-1}$ for [$C_{60}\subset$**3**], seemingly inconsistent with the previously reported TBTQ systems. Molecular dynamics (MD) simulations have been conducted for three different [$C_{60}\subset$TBTQ] complexes to resolve this. Because of the dominating dispersive interactions, the binding energies increase with the contact area between guest and host, however, only for rigid host structures. By means of free-energy calculations with an explicit solvent model it can be shown that the novel flexible TBTQ receptor **3** binds weakly because of hampering entropic contributions.

1. Introduction

In recent years the construction of nano-sized joints, motors, rotors, and machines has gained considerable interest. It has been lively discussed to which extent the design of macroscopic structures can be transferred to molecular dimensions.[1,2] On a macroscopic scale, fullerene C_{60} and its derivatives, in particular, represent features unmatched by any other compound serving as building block for molecular devices. The almost spherical molecules triggered the development of concepts targeting on the construction of nano-sized vehicles[3,4] and molecular motors.[5] As a fundamental building block of future molecular mechanical devices,[6] C_{60} (and its derivatives) might serve the purpose of the spherical ball head in a *simple* ball joint. In contrast to the majority of nano-sized rotors possessing a covalent single bond as rotation axis,[7] the design of a ball socket serving as stator of a nanorotor must fulfil several elaborate tasks. First of all, the mounting of nano-sized devices has to rely on the principle of self-assembly and the supramolecular complexes formed between the fullerene guest (e.g. C_{60}) and its receptor R must result in a complex of 1:1 stoichiometry from a thermally equilibrated solution. Because complex formation is a dynamic equilibrium process, the stability constant of the [$C_{60}\subset$R] complex has to be maximized to limit the fraction of (constantly) disassembling ball joints at the given experimental conditions. Conceptually, a sufficiently large activation barrier for the disassembly of [$C_{60}\subset$TBTQ] complexes might well serve this purpose because mechanically impacted ball joints would require "harsh" disassembly conditions (e.g. elevated pressure or temperature), thus mimicking the mechanical function of their macroscopic counterparts.

In earlier studies[8,9] we have presented a novel fullerene (C_{60}) host–guest system based on conformational inflexible and highly rigid tribenzotriquinacene (TBTQ) derivatives constituting the ball bearing (Figure 1, host **1** and host **2**). Here, host **1** represents a smaller variant, whereas **2** with its centrohexain-

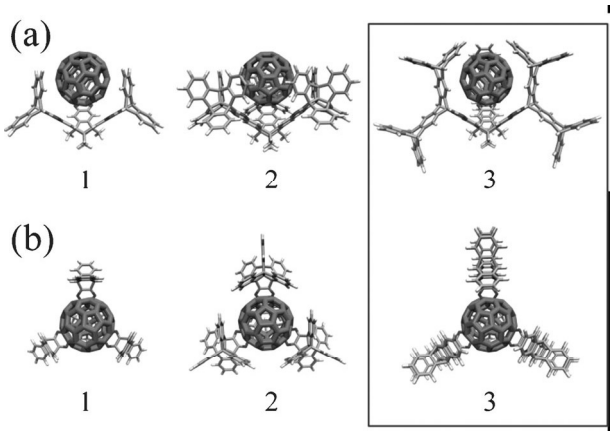

Figure 1. Schematic representation of [$C_{60}\subset$TBTQ] complexes with tribenzotriquinacene-based hosts **1**,[8] **2**[9], and **3:** a) side view and b) top view.

[a] *S. Henne, Dr. B. Bredenkötter, Prof. Dr. D. Volkmer*
Institute of Physics
Chair of Solid State and Materials Chemistry
Augsburg University, Universitätsstrasse 1
86159 Augsburg (Germany)
-augsburg
E-mail: dirk.volkmer@physik.uni

[b] *Dr. M. Alaghemandi, Dr. S. Bureekaew, Dr. R. Schmid*
Chair of Inorganic Chemistry 2
Computational Materials Chemistry Group
Ruhr University Bochum, Universitätsstrasse 150
44780 Bochum (Germany)

dane side arms has a perfect nearly semi-spherical shape leading to an enhanced contact surface area for dispersive binding of shape-complementary fullerene guests. To extend this series, we present here the novel TBTQ-based host **3**, which features an almost spherical cavity. This particular shape should exclusively lead to the formation of a [C_{60}⊂**3**] (1:1) host–guest complex with fullerene.

The aim of the present study is to assess how the refined design of the present TBTQ-based receptor **3** affects the interactions with C_{60} under realistic conditions, in order to develop guidelines for the future design of nano-devices based on self-assembling TBTQ-type receptors and fullerenes. In particular, we investigate the importance of surface area and molecular flexibility. In a combined experimental and theoretical investigation, the formation of three different [C_{60}⊂TBTQ] complexes (Figure 1) were analyzed with a special focus on the impact of conformational flexibility of receptor **3** on complex stability.

2. Results and Discussion

2.1. Synthesis of Receptor (3)

The TBTQ-based receptor **3** was synthesized through a trifluoroacetic acid (TFA) catalyzed condensation of hexaamino-tribenzotriquinacene **5**[10,11] with three equivalents of dione **9** (Scheme 1). To enable quantitative condensation, the reaction between **5** and **9** was carried out with an excess (4.5:1) of dione **9** with regard to hexamine **5**. The relatively low yield (35%) results from some difficulties encountered during the purification of the product from unreacted dione by preparative column chromatography. However, separating product **3** from a mixture of partially substituted triquinacenes proved to be a more difficult task, leading to even lower yields.

The ^{1}H NMR spectrum of the C_S symmetric *cis*-diol **8** (Figure S5 of the Supporting Information) shows two singlets at $\delta = 5.51$ and 5.50 ppm, which correspond to the four bridgehead protons of the triptycene moiety. Furthermore, the two central bridgehead protons correspond to the singlet at $\delta = 3.66$ and the two protons originating from vinylene carbonate relate to the singlet at $\delta = 4.13$ ppm.

The 20 aromatic protons correspond to four multiplets at $\delta = 7.42$–7.38, 7.31–7.27, 6.98–6.96, and 6.86–6.83 ppm. Owing to the C_{2v} point group symmetry of dione **9**, the four bridgehead protons of the triptycene moiety show only one singlet at $\delta = 5.37$ ppm in the ^{1}H NMR spectrum (Figure S6 f). The NMR spectra of receptor **3** (Figure 2) clearly confirm the C_{3v}-symmetry of the molecule (^{1}H NMR: 14 signals; ^{13}C NMR 26 signals). Note that the aromatic rings, which are annelated at the central 2.2.2-bicyclooctane moiety, are not chemically equivalent. This was also observed in similar tribenzotriquinacene-based host systems.[8,9,12] In detail, the six protons of the quinoxaline groups (a), the twelve *para* protons of the isolated benzene moieties (b, b′), the 18 bridgehead protons (g, h, h′), and the twelve protons of the four methyl groups at the tribenzotriquinacene moiety correspond to the singlets at $\delta = 7.68$, 7.43, 7.38, 5.26, 5.25, 5.19, 1.58, and 1.19 ppm, respectively. Since the benzene rings that are located at the top of the cage are very close to each other, the signals of the 12 *endo*, *endo* situated protons (d, f) show a high-field shift ($\delta = 7.11$–7.09, 6.61–6.59 ppm). The remaining 36 protons (c, c′) and (e, e′) relate to

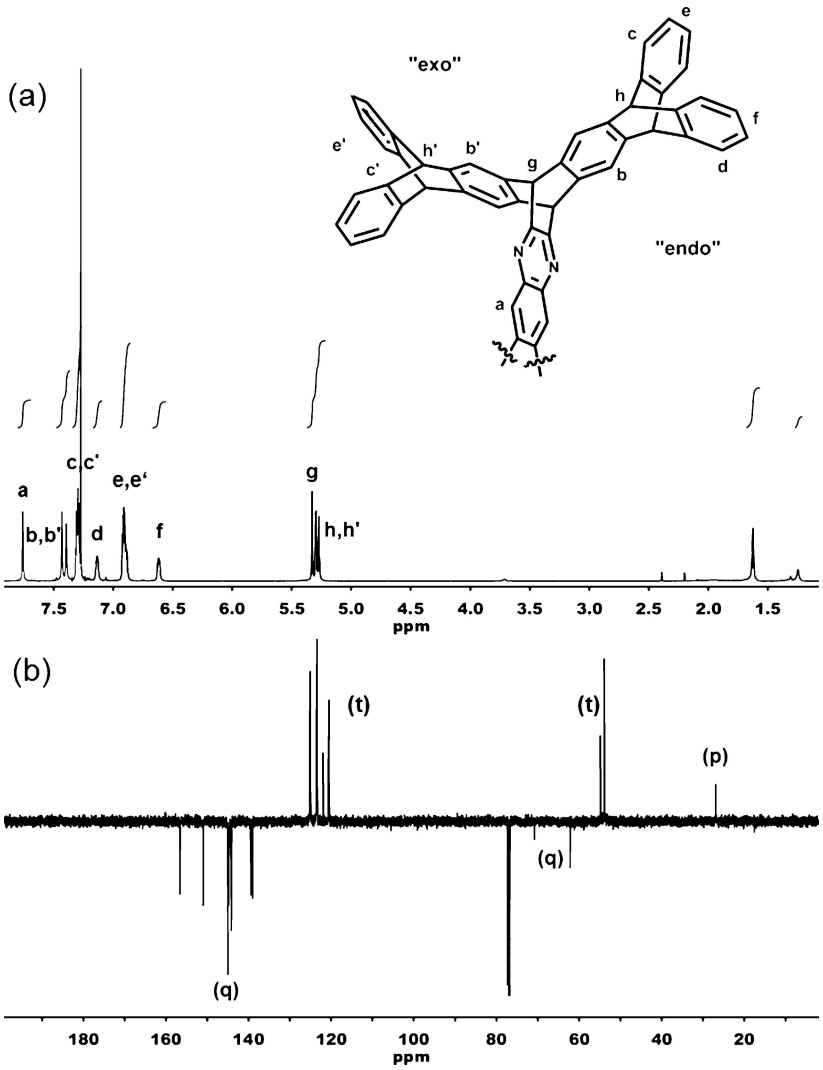

Figure 2. NMR spectra ($CDCl_3$, 300 K), of receptor 3: a) ^{1}H (500 MHz), b) ^{13}C-APT (100 MHz).

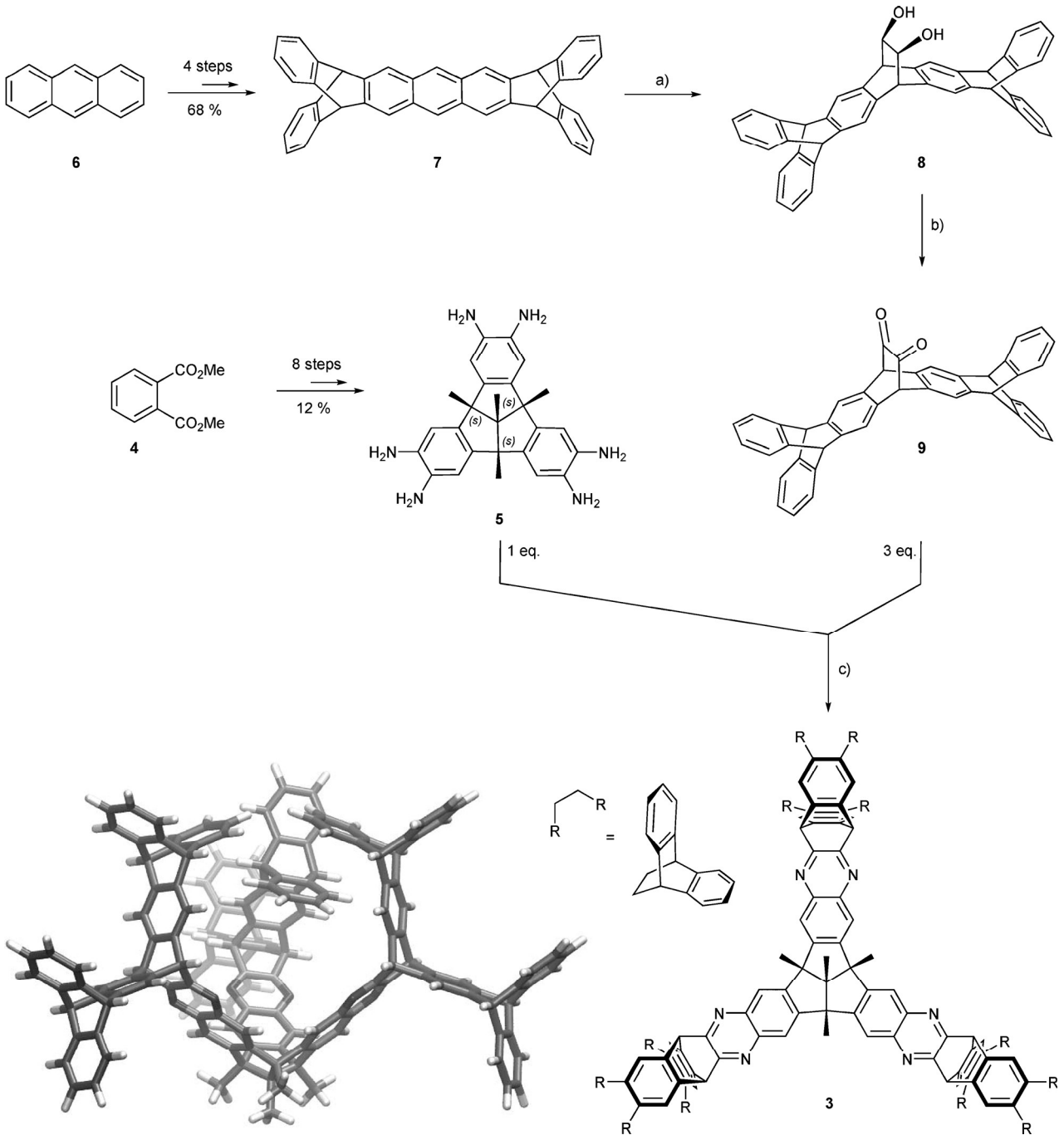

Scheme 1. Route for the synthesis of receptor **3**. Reaction conditions: a) 1. Vinylene carbonate, decahydronaphthalene, 190 °C, 48 h; 2. NaOH 40 %, EtOH/H_2O, 2 h; b) Swern oxidation: 1. $(COCl)_2$, DMSO/CH_2Cl_2, −60 °C; 2. NEt_3, 5 °C; c) *o*-dichlorobenzene, TFA cat., 100 °C, 48 h; Inset: 3D wire model of the tribenzotriquinacene-based receptor **3**.

two multiplets ($\delta = 7.25$–7.20, 6.88–6.83 ppm). This situation causes the observed high-field shift by magnetic shielding.

Similarly, the ^{13}C NMR spectrum of receptor **3** clearly confirms the C_{3v} symmetry of the molecule [the 66 quaternary carbon atoms ($\delta = 156$ to 139 ppm) correspond, as expected, to eleven signals; for the 66 tertiary aromatic carbon atoms ($\delta = 125$ to 120 ppm) only nine signals are detected]. The 26 aliphatic carbon atoms relate to six signals. The signal for the central methyl group is, comparable to other tribenzotriquinacens, not detectable.[13]

2.2. Formation of Host–Guest Complexes between Receptor 3 and C_{60}

To our surprise, all efforts initially failed to encapsulate C_{60} in the cavity of receptor **3**. Analogous host–guest complexes can be generally prepared, isolated, purified, and characterized, if a mixture of the host and an excess of guest (=fullerene) molecules are dissolved and heated in a high-boiling solvent to reach the thermodynamic equilibrium.[14] To verify the above-mentioned experimental findings, we performed mass spec-

trometry investigations because it is well known that host–guest complexes are detectable by using mild ionization techniques, such as electrospray ionization (ESI) or matrix-assisted laser desorption/ionization (MALDI).

Employing a mixture of host **3** and a tenfold excess of C_{60}, the anticipated complex fragment ($[C_{60}\subset\mathbf{3}+H]^+$, calcd *m/z*= 2799) was not detectable, while the analogous experiment with receptor **2** led to mass-spectrometry-detectable ionized 1:1 host–guest complexes.[9] The absence of a fragment that could be assigned to $[C_{60}\subset\mathbf{3}]$ does not rigorously exclude the existence of such complexes in solution, but it may indicate that van der Waals (vdW) interactions are substantially weakened, as the entropic driving force for dissociation of weakly bound molecular complexes in the gas phase is in many cases too high.[15] In the MALDI mass spectrum of the reaction mixture (Figure 3), apart from the monomer ($[\mathbf{3}+H]^+$, calcd *m/z*=

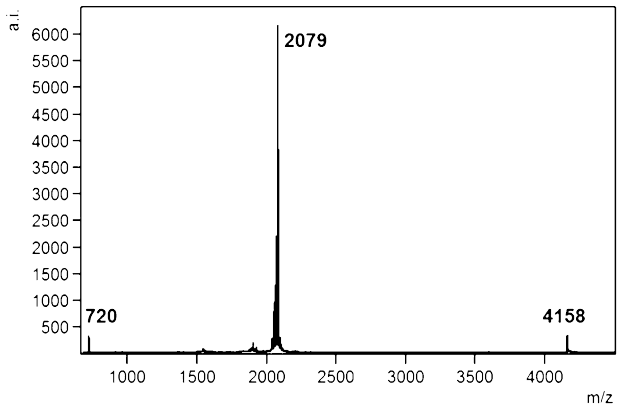

Figure 3. Mass spectrum (MALDI-TOF) of a mixture of receptor **3** and C_{60} (1:1).

2079) and fullerene ($[C_{60}]^+$, calcd *m/z*=720) the mass fragments accounting to the dimer ($[\mathbf{3}+H]^+$ calcd *m/z*=4158) are observed. This is in line with the results for a recently developed chiral tribenzotriquinacene-based host, which has a similar low $[C_{60}\subset$host] stability constant of $319\pm156\ M^{-1}$.[12]

Based on these findings we performed ^1H NMR titration experiments to determine the stoichiometry and the stability constant of the host–guest complex $[C_{60}\subset\mathbf{3}]$. All investigations were performed with a solvent mixture of $CDCl_3$ and CS_2 (1:1), which allows us to compare results from the present study with the corresponding complex stability constants from previous investigations.[8,9,12] The signal of the *endo*, *endo* situated *ortho* protons (f, δ=6.61–6.59 ppm) can be evaluated while the other signals provide insufficient differences in the chemical shift. To take experimental artefacts of non-specific complex formation[16] such as non-linearity[17] or self-aggregation[18,19] into account, the validity of the Beer–Lambert law, which is a linear dependence of the absorbance on the solute's concentration, was tested for pure solutions of host **3** in the appropriate concentration regime within a first set of experiments, but such artefacts were not detected.

The method of continuous variation (Job plot)[20] was applied to determine the stoichiometry of the complex(es)

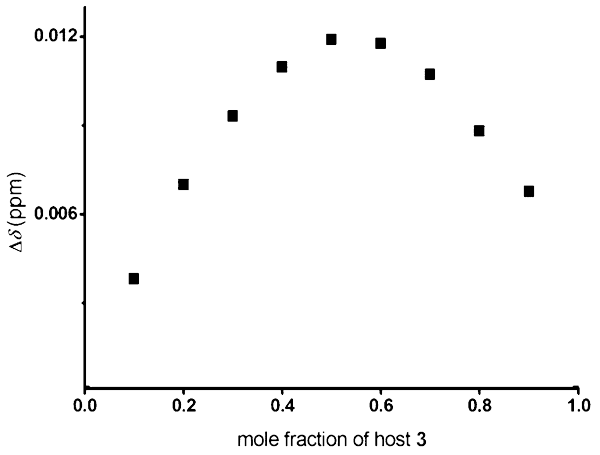

Figure 4. Job plot showing the 1:1 stoichiometry of host **3** versus C_{60} in solution (chloroform-d_1, 300 K, δ=6.5979 ppm); overall concentration ($[\mathbf{3}]+[C_{60}]$)=4.8 10^{-4} mol L^{-1}.

formed between host **3** and C_{60} (Figure 4), and the expected 1:1 relationship was thus detectable.

The quantitative association constant was determined by the procedure outlined by Conners.[21] For this purpose the ^1H NMR shift of a suitable signal of receptor **3** (*endo*, *endo* situated *meta* protons) was plotted against the guest concentration, and the individual association constant was fitted by a non-linear regression, leading to an equilibrium constant of $K_1=213\pm37\ M^{-1}$ (Figure 5). This is an averaged value from three independent ^1H NMR titration experiments. In a typical experiment, 0.15 equivalent portions of C_{60} were added to a constant concentration of receptor **3** (1.0×10^{-3} M). Upon addition of C_{60}, the mutual magnetic shielding of the exposed protons increases, and therefore, a rising high-field shift was observed.

The very low complex stability constant reported in the present study is not consistent with our earlier findings on complex formation of C_{60} with structurally less-evolved TBTQ-

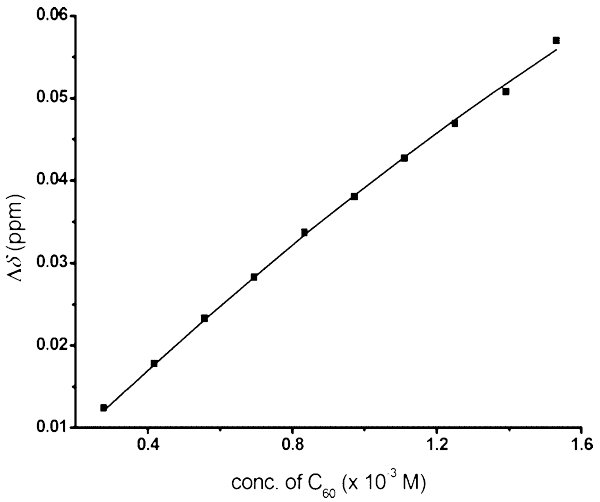

Figure 5. Nonlinear curve regression of the titration of receptor **3** (1.0×10^{-3} mol L^{-1}) with C_{60}. ^1H NMR shift determined at δ=6.5979 ppm.

based hosts **1**[8] and **2**,[9] but stands in good agreement with results from similar investigations employing a novel TBTQ-based chiral host.[12] The complex stability constant of [C_{60}⊂**3**] is smaller by more than an order of magnitude compared to the first-generation host **1**[8] ($K_1 = 2908 \pm 360\ M^{-1}$). This discrepancy is even more pronounced for the centrohexaindane-extended receptor **2**,[9] whose complex stability constant ($K_1 = 14550 \pm 867\ M^{-1}$) is 70 times larger than that of receptor **3**.

Table 1. Binding energies of the [C_{60}⊂TBTQ] 1:1complexes in the gas phase.

E_{form}(FF) [kJ mol^{-1}]	[C_{60}⊂**1**] MM3[9]	MOF-FF (this work)	[C_{60}⊂**2**] MM3[9]	MOF-FF (this work)	[C_{60}⊂**3**] DFT + D[a]	DFT + D/Solv.[b]	MOF-FF (this work)
$T = 0$ K	−157	−143	−226	−221	−145	−142	−173
$T = 300$ K		−140		−180			−128

[a] DFT with dispersion correction (B97 + D2).[22] [b] DFT with dispersion correction (B97 + D2) and COSMO solvation model.[23]

Because of these facts, we decided to combine these experimental results with theoretical investigations to assess how the design of TBTQ-based receptors affects fullerene binding under realistic conditions to develop design guidelines targeting on self-assembling TBTQ-type receptors and fullerenes displaying maximum stability and assembly efficiency.

2.3. Theoretical Investigation on Complexes of Receptors 1, 2, and 3 Formed with C_{60}

The overall complex stability is determined by the free energy of complexation, which can be separated into three major contributions: the (mainly dispersive) attractive interaction between host and guest, characterized by the amount of contact surface area, the repulsive deformation energy determined by the host's flexibility (rigidity), and entropic contributions. Note that the latter are dominated by the loss of translational entropy of the guest, but for a flexible host also internal degrees of freedom can get locked upon complexation. In addition, the solvent interactions with both host and guest affect the complexation process. For example, the attractive dispersive host–guest interaction, present in the gas phase, is diminished by the loss of dispersive stabilization from the solvent. To shed light on the interplay of these effects, we performed a number of different atomistic calculations of the complexation process. First, we used molecular mechanics (MM) and a first-principles derived force field (MOF-FF[30]), to calculate the binding energy of the complexes at zero-point energy, where no thermal fluctuations of the host molecules are taken into account. In the second step, molecular dynamics simulations (MD) were carried out to study the influence of entropic contributions on the binding energy. In the numerically most demanding case, an explicit solvent model has been included to take into account all enthalpic and entropic contributions ascribable to the solvent.

In our previous work on receptors **1** and **2**, an MM3-based force field was used,[9] which was validated with respect to dispersion-corrected density functional theory (DFT) computations; the results could corroborate the experimental findings. In this work, we used the new force field MOF-FF,[30] developed in a different context, which was explicitly parameterized by a genetic algorithm approach for receptors **1** to **3**, based on a dispersion-corrected DFT-computed reference data. As a consequence, the new force field more accurately describes the most relevant strain energy for a deformation of **3**. The gas-phase C_{60} binding energies of the three studied TBTQ hosts **1** to **3** are summarized in Table 1. For comparison, the results of the previous studies are also included in this table. Because of reparameterization, the results of the previous FF calculations for **1** and **2** are slightly different from the data computed in this work.

However, the binding energies calculated based on MOF-FF indicate that the magnitude of the binding energy of the [C_{60}⊂**3**] complex is lower than that of **2**, but higher in comparison with the value of [C_{60}⊂**1**], in contrary to the experimental complex stability constants. As expected, the larger contact area of **3** as compared to **1** leads to a stronger C_{60} binding, neglecting any solvent and entropy contributions. Interestingly, by including finite temperature effects via MD simulations at 300 K alone [E_{form}(MD), difference of averaged potential energies], the binding energy of [C_{60}⊂**3**] is slightly smaller in magnitude than for host **1**. It should be noted that in contrast to the rather stiff receptors **1** and **2**, in the case of receptor **3**, a strong deformation upon inclusion of C_{60} into the receptor's cavity is observed.

Figure 6 shows the relaxed structure of **3** with and without C_{60}. To reduce the strain of the three "arms" touching each other on top of the erected cavity, and to increase the dispersive π–π interactions, the minimum-energy structure folds into a conformer that breaks the C_{3v} point group symmetry. The symmetry is recovered when the spherical C_{60} guest molecule occupies the host cavity (see Figure 6 b). Accordingly, a substantial deformation of the free host is needed to provide the necessary space for C_{60}. As a consequence, the binding energy (128 kJ mol^{-1}) is lower than the 140 and 180 kJ mol^{-1} computed for hosts **1** and **2**, respectively. As already mentioned, this

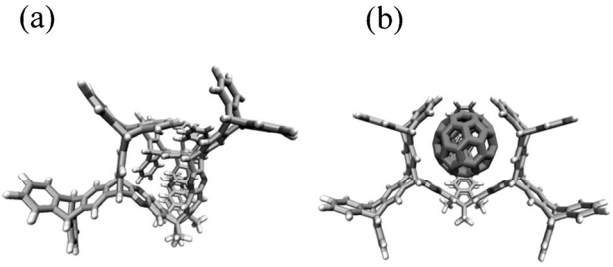

Figure 6. Structures of the free host **3** (a) and the 1:1 fullerene complex [C_{60}⊂**3**] (b).

results from the preorganization energy needed to deform host **3** into the proper structure.

The theoretical calculations discussed up to now were carried out in the gas phase. To explicitly investigate the effect of solvent molecules, we performed MD simulations of each host and its fullerene complex embedded in a solvent box of 1000 benzene molecules in a canonical ensemble at 300 K. To keep the parametrization of the force field tractable, we decided to use benzene as the solvent in contrast to the solvent mixture of $CHCl_3/CS_2$ used in the experimental investigations. This could be justified in light of the scope of our study, which is expected to glean qualitative trends rather than a fully quantitative prediction of complex stability constants. Figure 7 shows a schematic view of the simulation box of host **3** with C_{60}. The binding energy and binding free energy (ΔG) results of the complexes in solution are given in Table 2.

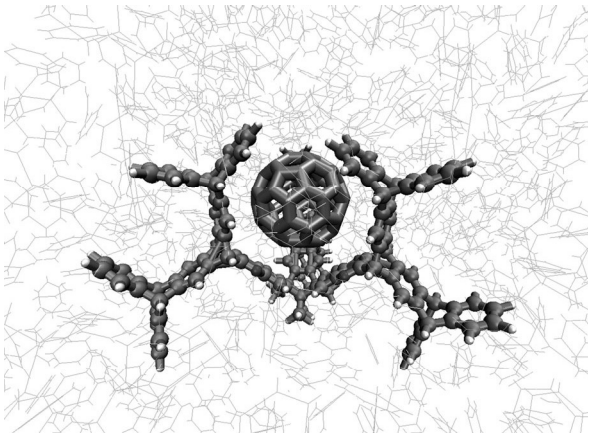

Figure 7. Schematic representation of the simulation box of a [C_{60}⊂**3**] complex embedded in a solvent box of 1000 benzene molecules.

Table 2. Binding energies and ΔG of complex formation for the 1:1 [C_{60}⊂host] complexes in benzene.

	[C_{60}⊂**1**]	[C_{60}⊂**2**]	[C_{60}⊂**3**]
E_{form}(MD) [kJ mol^{-1}]	−17.25	−49.03	−0.60
ΔG [kJ mol^{-1}]	−29.8	−67.5	−21.8

Here, the binding energy was calculated by the difference of the averaged potential energy from two different configurations, first when the distance of the host and C_{60} is around its equilibrium value and second when the distance between the center of mass of two objects is about 25 Å. Note that these binding energies include all enthalpic contributions from host, guest, and solvent, but no entropic contributions.

First of all, all the values are substantially smaller than the gas-phase results, indicating a strong competition for the dispersive interactions. Surprisingly, the binding energy of host **3** is much smaller than the corresponding values of the two other more rigid receptors **1** and **2**. However, such a difference of an averaged energy is largely affected by statistic errors and should not be over-interpreted in this case. It should also be noted that the DFT calculations with an implicit solvent model (DFT + D/Solv) shown in Table 2 do not indicate a significant difference from the corresponding gas-phase results, and the binding energies are far from those computed by MD simulations with an explicit solvent. To summarize, the solvent molecules play a significant role in the complexation process and an explicit solvent model is needed for a proper theoretical treatment of these systems. Up to this point, however, entropic contributions have not been taken into account. In addition, the necessary deformation upon complex formation in case of host **3** raises the question whether a kinetic barrier could exist, preventing the formation of the fullerene–host complex. To verify this question, and to compute the free energy of binding, we performed potential of mean force (PMF) calculations for each complex in the presence of solvent molecules by a "slow growth" thermodynamic integration (TI) approach.[24] To compute the PMF, the center of mass of the C_{60} guest and the host were constrained to a certain distance. The constraint was slowly moved from a value just below the equilibrium distance to large values with solvent-separated host and guest, integrating the force acting on it to give the accumulated work or PMF. We used a growth rate of $v = 0.001$ Å ps^{-1} in this work. Figure 8 shows the accumulated work versus the relative

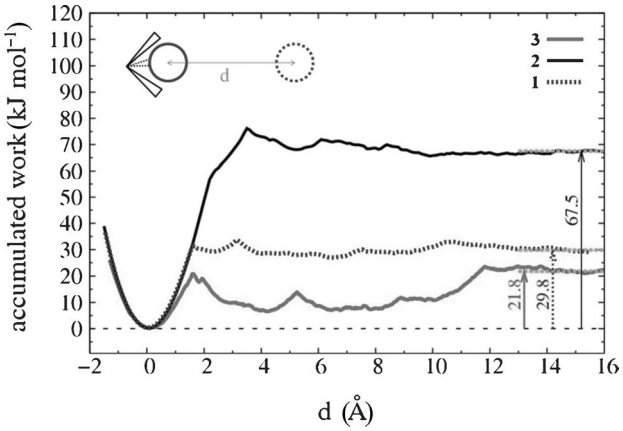

Figure 8. Accumulated work versus relative distance from the equilibrium position (d) of C_{60} and the hosts' **1–3** center of mass.

distance from the equilibrium position (d) of C_{60} and the host's center of mass. As expected, the minimum of the PMF curve is located for all three complexes at the position where the host and C_{60} are found at their equilibrium distances. At closer distances, repulsive interactions lead to a sharp increase of the PMF. On the other hand, increasing the distance between host and C_{60} also enhances the accumulated energy, indicating a destabilization of the system. This results from the steric hindrance of the host and a loss of dispersive interactions with the guest, which is only partly compensated by an inflow of solvent molecules into the host's binding cavity. Despite the larger contact area of **3** as compared to **1**, this "barrier" of decomplexation (21 kJ mol^{-1}) is the lowest for **3**. The high conformational flexibility increases the entropy in the uncomplexed

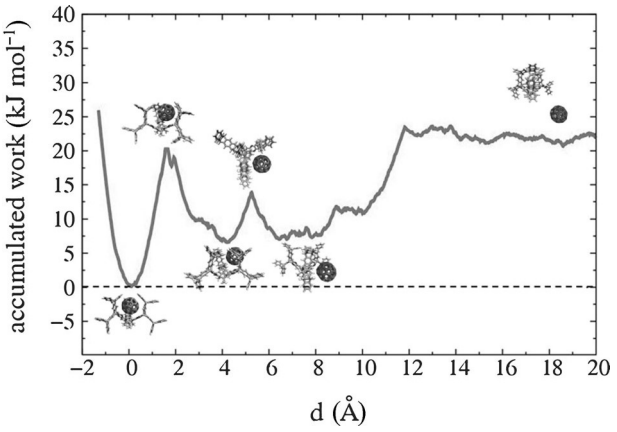

Figure 9. Accumulated work versus distance from the equilibrium position (d) for the [C_{60}⊂**3**] complex.

state of **3**. In addition to that, only for **3**, further local minima in the distance between approximately 1.8 and 4.1 Å are observed. These minima correspond to the complexation of C_{60} in the outer pockets of the arms of host **3**. In Figure 9, the PMF of host **3** is shown at higher resolution, with snapshots of the complex structure at certain characteristic points. The key values for a comparison of different host–guest complexes are the relative PMF values at distances where there is no interaction between host **3** and C_{60}; indicated by the vertical arrows in Figure 8.

This relative energy, which is the negative of the free energy of complex formation, is smaller for host **3** (with a value of about 21.8 kJ mol^{-1}) compared to the other hosts, **1** and **2**. The corresponding value of host **1** (29.8 kJ mol^{-1}) is above that of host **3**, but much lower than the value of host **2** (67.5 kJ mol^{-1}). For comparison, the ΔG^{exp} values, derived from the measured complex stability constants of 20, 24, and 13 kJ mol^{-1} for receptors **1**, **2**, and **3**, respectively, show the same ordering. Thus, only by including both an explicit solvent model and entropic contributions do the theoretical simulations qualitatively reproduce the experimental trends. Similar absolute deviations between experimental and theoretical complexation free energies for supramolecular complexes have recently been reported using a continuum approach for the solvation effects.[25] Note that especially for weakly complexing systems, the errors in ΔG^{exp} can be large. Furthermore, in MD simulations, a different solvent was used, as compared to the NMR-titration experiments, which could explain the rather large deviations for **2**.[26] Overall, the enhanced flexibility of host **3** does not lead to a constrictive binding mode[27] with a large barrier for complex formation, as might be anticipated. In contrast, the available degrees of freedom make complex formation less probable for entropic reasons and the necessary deformation to adopt to the guest.

3. Conclusions

In summary, we have synthesized an extended tribenzotriquinacene-derived host molecule (**3**) with an almost closed cavity, optimized for fullerene C_{60}. As expected, this led to the favored 1:1 complex formation with C_{60}, but surprisingly, the resulting complex stability constant $K = 213$ L mol^{-1} was much lower than the corresponding values for some recently reported, more rigid host systems, despite the larger contact area of **3**. The reason for this counterintuitive behavior could only be revealed by atomistic molecular dynamics simulations with an inclusion of explicit solvent effects. For an accurate representation of the deformation energy, the first-principles-parameterized force field MOF-FF was extended to describe the rigid hosts **1** and **2**, as well as the new flexible **3** system. The simulations indicate that the necessary deformation energy of the flexible **3** to accommodate the C_{60} already reduces its complexation strength. More importantly, a computation of the potential of mean force in an explicit solvent box is needed in the theoretical treatment to capture all entropic and solvent effects. Our combined experimental and theoretical investigation demonstrates that for a rational design of self-assembling molecular rotors, over-simplifying concepts derived from macroscopic objects are insufficient and aspects such as entropy contributions from locked degrees of freedom or explicit solvent–molecule interactions can have a detrimental effect and always need to be considered. On the other hand, accurate atomistic models can be used as a predictive tool to aid the design of such complex molecular systems.

Experimental Section

Experimental Details

Melting points (uncorrected): OptiMelt, MPA 100 apparatus. Infrared (IR) spectra: Bruker FTIR IFS 113v spectrometer; KBr pellets. NMR spectroscopy: Bruker DRX 500 or Bruker Avance 400; data given as ppm; *J* values are given in Hz; spectra referenced to the residual solvent peak; the degree of substitution of C atoms was determined by the APT or DEPT method. MALDI-TOF mass spectra: Bruker, Daltonics REFLEX III. N_2-laser (337 nm), pulsed ion extraction (PIE), HIMAS-detector, acceleration voltage 20 kV, matrix: DHB. Thin-layer chromatography: Silica gel (Kieselgel F_{254}) on Al foils (Merck). Gravity column chromatography: Silica gel (Kieselgel 60, 0.063–0.2 mm, Merck). All solvents were purified by distillation before use and dried according to standard procedures.

***Cis*-5,7,9,14,16,18-hexahydro-5,18:9,14-bis([1,2]benzeno)-7,16-ethanoheptacene-25,26-diol (8):** A suspension of pentiptycene **7**[28] (1.0 g, 1.9 mmol) and vinylene carbonate (6.5 g, 72.1 mmol) in decahydronaphthalene (25 mL) was heated in an autoclave at 190 °C for three days. The solvent was removed under reduced pressure and the brownish residue was heated under reflux in a mixture of ethanol (50 mL) and NaOH (40 %, 20 mL) for two hours. The resulting solid was filtered by suction, washed with water and ethanol, and dried in vacuum. Subsequently, the residue was recrystallized from dichloromethane to yield diol **8** (0.9 g, 85 %) as a slightly brown powder. M.p. 322 °C (dec). IR [ν (cm^{-1})]: 3529.1, 3456.7, 3068.4, 3015.8, 2945.1, 2924.4, 1618.8, 1456.3, 1405.7, 1190.6, 1085.6, 1009.5, 738.7. ^{1}H NMR [400 MHz, [D_6]DMSO (dimethyl sulfoxide), δ (ppm)]: 7.42–7.38 (m, 4 ArH), 7.31–7.27 (m, 8 ArH), 6.98–6.96 (m, 4 ArH), 6.86–6.83 (m, 4 ArH), 5.51 (s, 2 H), 5.50 (s, 2 H), 4.13 (s, 2 H), 3.66 (s, 2 H). MS (MALDI-TOF): $m/z = 613$ $[M + Na]^+$. Elemental analysis: calc. (%): C 89.46, H 5.12; found: C 89.08, H 5.08.

5,7,9,14,16,18-Hexahydro-5,18:9,14-bis([1,2]benzeno)-7,16-ethanoheptacene-25,26-dione (9): Oxalyl chloride (0.2 mL, 2.3 mmol) was added under argon at −78 °C to a mixture of dry DMSO (0.2 mL, 2.8 mmol) and dry CH_2Cl_2 (5 mL), and the resulting solution was stirred for 15 min. Subsequently, a solution of diol **8** (590 mg, 1.0 mmol) in dry CH_2Cl_2/DMSO (7:3, 200 mL) was added over a period of 1.5 h and the resulting mixture was stirred for 60 min at −78 °C. Then, triethylamine (0.8 mL, 5.7 mmol) was added slowly and the reaction mixture was stirred at 5 °C for 1.5 h and poured subsequently in 2 M HCl (50 mL). After the evolution of gas had stopped, the organic layer was separated and the aqueous phase was extracted five times with CH_2Cl_2. The combined organic layers were washed three times with water and dried with sodium sulfate. The solvent was evaporated and the residue was recrystallized from *n*-pentane to yield dione **9** (467 mg, 80%) as a yellow powder. M.p. 239 °C (dec). IR [ν (cm^{-1})]: 3065.8, 3039.8, 3018.1, 2956.6, 1731.3, 1479.6, 1263.6, 1156.5, 906.3, 738.0, 625.6. ^{1}H NMR [400 MHz, $CDCl_3$, δ (ppm)]: 7.42–7.40 (m, 4 ArH), 7.32–7.30 (m, 4 ArH), 7.20 (s, 4 ArH), 7.06–7.04 (m, 4 ArH), 6.92 −6.90 (m, 4 ArH), 5.37 (s, 4H), 4.64 (s, 2H). ^{13}C NMR [100 MHz, $CDCl_3$, δ (ppm)]: 183.1, 146.7, 144.6, 144.4, 131.6, 125.5, 125.3, 123.8, 123.6, 121.3, 59.0, 53.7. MS (MALDI-TOF): $m/z = 530$ $[M-C_2O_2]^{+\cdot}$. Elemental analysis: calc. (%) for $C_{44}H_{26}O_2 \cdot CHCl_3 \cdot H_2O$ (724.06): C 74.64, H 4.03; found: C 74.36, H 4.07.

Receptor (3): was added (under argon) to a solution of hexamine **5**[10] (40 mg, 94 μmol) and dione **9** (250 mg, 425 μmol) in *o*-dichlorobenzene (50 mL) and a catalytic amount of trifluoroacetic acid; the mixture was subsequently stirred at 100 °C for 60 h. The solvent was removed and the residue was purified by column chromatography (gradient: chloroform to chloroform/methanol 10:1) to get host **3** (67 mg, 35%) as a white powder. M.p. 212–213 °C. IR [ν (cm^{-1})]: 3445.5, 3066.3, 3016.9, 2958.7, 2924.8, 2854.9, 2356.5, 2328.5, 1673.0, 1488.4, 1455.3, 1374.5, 1182.5, 1151.8, 886.0, 741.8. ^{1}H NMR [400 MHz, $CDCl_3$, δ (ppm)]: 7.68 (s, 6 ArH), 7.43 (s, 6 ArH), 7.38 (s, 6 ArH), 7.25–7.20 (m, 18 ArH), 7.11–7.09 (m, 6 ArH), 6.88–6.83 (m, 18 ArH), 6.61–6.59 (m, 6 ArH) 5.26 (s, 6H), 5.25 (s, 6H), 5.19 (s, 6H), 1.58 (s, 9H), 1.19 (s, 3H). ^{13}C NMR [100 MHz, $CDCl_3$, δ (ppm)]: 156.5 (q), 150.9 (q), 145.0 (q), 144.9 (q), 144.7 (q), 144.2 (q), 144.1 (q), 139.4 (q), 139.0 (q), 138.9 (q), 125.2 (t), 125.1 (t), 125.1 (t), 125.0 (t), 123.5 (t), 123.4 (t), 123.3 (t), 121.9 (t), 120.5 (t), 70.7 (q), 62.1 (q), 54.7 (t), 53.8 (t), 53.8 (t), 26.9 (p), one primary carbon atom cannot be detected; MS: (MALDI-TOF): $m/z = 2079$ $[M+H]^+$, 4158 $[2M+H]^+$. Elemental analysis: calc. (%) for $C_{158}H_{96}N_6 \cdot 6\ H_2O$ (2186.58): C 86.78, H 4.97, N 3.84; found: C 86.79, H 5.13, N 3.95.

Computational Details

In this study, the parameterization scheme for optimizing the force field is based on the building block approach, which means, for computational reasons, that the big host molecules are subdivided into the smaller parts (segments), see Figure 10. Considering the benzene molecule as a reference origin, the force-field parameters for each segment are generated. Please note that host **1** is combined from segments a and b. Host **2** contains segments a and c. And finally, host **3** is made from a combination of segments a, b, and d, shown in Figure 10. The model segments were completely optimized and the Hessian matrix was computed using the TURBOMOLE (V6.3) package.[29] The hybrid functional B3LYP[30] was used throughout. A finer numerical integration grid ("m5") was employed to improve the computed low-frequency normal modes. For main-group elements (C, H, N, O), cc-pVDZ basis sets were used.[31] The effective atomic charges were obtained from a fit of the electrostatic potential (ESP) by the Merz–Kollman sampling scheme.[32] We modified the charges resulting from the ESP fit to generate "neutral hosts". VdW interaction terms in the force field are taken from the work by Allinger et al.[33] After defining the non-bonded terms, the genetic algorithm (GA) optimizer is used to optimize the parameter set of bonded terms in the force field. Since the benzene molecule has been previously parameterized, in the fitting procedure, those internal coordinates of benzene are not included. For details of the force-field parameterization, we refer to Ref. [34].

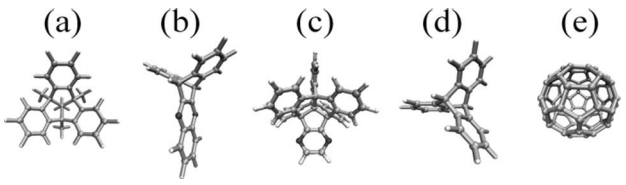

Figure 10. Sub-parts of the host–guest systems shown in Figure 1. Host **1** is made of a combination of fragments a and b, **2** of a, b, and c, and **3** is made of a, b, and d.

All MD simulations were carried out using our in-house-developed *pydlpoly* package, which is an extension of DL POLY Classic.[35] A temperature of 300 K was used for all the MD calculations. A Nosé–Hoover thermostat[361] with a coupling time of 1 ps was adopted to guarantee a constant temperature. Time steps of 1 fs were employed. Non-bonded interactions were evaluated from a Verlet neighbor list. A cutoff radius of 1.1 nm was adopted while the neighbor list cutoff was 1.2 nm.

Acknowledgements

We gratefully acknowledge the financial support provided by the German Science Foundation (DFG Vo829/6–1, DFG SCHM 1389/5–1).

Keywords: binding energy · buckyballs · computational chemistry · molecular devices · self-assembly

[1] a) V. Balzani, M. Gómez-López, J. F. Stoddart, *Acc. Chem. Res.* **1998**, *31*, 405–414; b) V. Balzani, A. Credi, F. M. Raymo, J. F. Stoddart, *Angew. Chem. Int. Ed.* **2000**, *39*, 3348–3391; *Angew. Chem.* **2000**, *112*, 3484–3530–3391; c) *Top. Curr. Chem.* **2005**, *262*, special volume on Molecular Machines (Ed.: T. R. Kelly); d) H. Liu, J. Xu, Y. Li, Y. Li, *Acc. Chem. Res.* **2010**, *43*, 1496–1508; e) W. Yang, Y. Li, H. Liu, L. Chi Y. Li, *Small* **2012**, *8*, 504–516.

[2] E. R. Kay, D. A. Leigh, F. Zerbetto, *Angew. Chem. Int. Ed.* **2007**, *46*, 72–191; *Angew. Chem.* **2007**, *119*, 72–196.

[3] Y. Shirai, A. J. Osgood, Y. Zhao, K. F. Kelly, J. M. Tour, *Nano Lett.* **2005**, *5*, 2330–2334.

[4] T. Sasaki, J.-F. Morin, M. Lu, J. M. Tour, *Tetrahedron Lett.* **2007**, *48*, 5817–5820.

[5] N. Koumura, R. W. Zijlstra, R. A. van Delden, N. Harada, B. L. Feringa, *Nature* **1999**, *401*, 152–155.

[6] a) F. Diederich, M. Gómez-López, *Chem. Soc. Rev.* **1999**, *28*, 263–277; b) T. Seidemann, *J. Phys. Condens. Matter* **2003**, *15*, 521–549; c) N. Martin, J.-F. Nierengarten, *Tetrahedron* **2006**, *62*, 1917–1961.

[7] a) O. S. Akkerman, J. Coops, *Recl. Trav. Chim. Pays-Bas* **1967**, *86*, 755–761; b) F. Cozzi, A. Guenzi, C. A. Johnson, K. Mislow, W. D. Hounshell, J. F. Blount, *J. Am. Chem. Soc.* **1981**, *103*, 957–958; c) B. L. Feringa, W. F. Jager, B. de Lange, A. W. Meijer, *J. Am. Chem. Soc.* **1991**, *113*, 5468–5470; d) T. C. Bedard, J. S. Moore, *J. Am. Chem. Soc.* **1995**, *117*, 10662–10671; e) T. R. Kelly, H. De Silva, R. A. Silva, *Nature* **1999**, *401*, 150–152; f) T. E. Glass, *J. Am. Chem. Soc.* **2000**, *122*, 4522–4523; g) T. R. Kelly, R. A. Silva, H. De Silva, S. Jasmin, Y. Zhao, *J. Am. Chem. Soc.* **2000**, *122*, 6935–

6949; h) B. L. Feringa, R. A. van Delden, N. Koumura, E. M. Geertsema, *Chem. Rev.* **2000**, *100*, 1789 – 1816; i) S. Toyota, T. Iida, C. Kunizane, N. Tanifuji, Y. Yoshida, *Org. Biomol. Chem.* **2003**, *1*, 2298 – 2302; j) S. Toyota, T. Makino, *Tetrahedron Lett.* **2003**, *44*, 7775 – 7778; k) D. A. Leigh, J. K. Y. Wong, F. Dehez, F. Zerbetto, *Nature* **2003**, *422*, 759 – 765.

[8] B. Bredenkötter, S. Henne, D. Volkmer, *Chem. Eur. J.* **2007**, *13*, 9931 – 9938.

[9] S. Henne, B. Bredenkötter, A. A. Dehghan Baghi, R. Schmid, D. Volkmer, *Dalton Trans.* **2012**, *41*, 5995 – 6002.

[10] J. Tellenbröker, D. Kuck, *Angew. Chem. Int. Ed.* **1999**, *38*, 919 – 922; *Angew. Chem.* **1999**, *111*, 1000 – 1004.

[11] a) W. A. Moser, R. W. Soeder, *J. Org. Chem.* **1971**, *36*, 1561 – 1563; b) D. Kuck, *Chem. Rev.* **2006**, *106*, 4885 – 4925.

[12] B. Bredenkötter, M. Grzywa, M. Alaghemandi, R. Schmid, W. Herrebout, P. Bultinck, D. Volkmer, *Chem. Eur. J.* DOI: 10.1002/chem.201304980.

[13] D. Kuck, A. Schuster, R. A. Krause, J. Tellenbröker, C. P. Exner, M. Penk, H. Bögge, A. Müller, *Tetrahedron* **2001**, *57*, 3587 – 3613.

[14] a) K. N. Houk, K. Nakamura, C. M. Sheu, A. E. Keating, *Science* **1996**, *273*, 627 – 629; b) X. Wang, K. N. Houk, *Org. Lett.* **1999**, *1*, 591 – 594; c) D. J. Cram, M. E. Tanner, C. B. Knobler, *J. Am. Chem. Soc.* **1991**, *113*, 7717 – 7727; d) D. J. Cram, M. T. Blanda, K. Paek, C. B. Knobler, *J. Am. Chem. Soc.* **1992**, *114*, 7765 – 7773.

[15] M. D. Pluth, K. N. Raymond, *Chem. Soc. Rev.* **2007**, *36*, 161 – 171.

[16] W. G. Barb, *Trans. Faraday Soc.* **1953**, *49*, 143 – 148.

[17] C. W. Davis, Ion Association, Butterworth, Washington, D. C., **1962**, 41.

[18] H. J. Schneider, A. Yatsimirsky, *Principles and Methods in Supramolecular Chemistry*, Wiley, Chichester, **2000**, 137 – 221.

[19] B. Dodson, R. Foster, A. A. S. Bright, M. I. Foreman, J. Gorton, *J. Chem. Soc. B* **1971**, 1283 – 1293.

[20] A. Job, *Ann. Chim.* **1929**, *9*, 113.

[21] K. A. Connors, Binding Constants, John Wiley, New York, **1987**.

[22] S. Grimme, *J. Comput. Chem.* **2006**, *27*, 1787 – 1799.

[23] A. Klamt, G. Schürmann, *J. Chem. Soc. Perkin Trans. 2* **1993**, *2*, 799 – 805.

[24] J. Schlitter, *Eur. Phys. J.: Spec. Top.* **2011**, *200*, 91 – 105.

[25] S. Grimme, *Chem. Eur. J.* **2012**, *18*, 9955 – 9964.

[26] For the simulations, benzene was used as a solvent to keep the parameterization effort tractable. However, in benzene both components are insoluble and a $CDCl_3/CS_2$ solvent mixture was used in the NMR experiments.

[27] L. C. Quan, D. J. Cram, *J. Am. Chem. Soc.* **1991**, *113*, 2754 – 2755.

[28] H. Hart, A. Bashir-Hashemi, J. Luo, M. A. Meador, *Tetrahedron* **1986**, *42*, 1641 – 1654.

[29] TURBOMOLE V6.3 2011, a development of University of Karlsruhe and-Forschungszentrum Karlsruhe GmbH, 1989 – 2007, TURBOMOLE GmbH, since 2007 available from http://www.turbomole.com.

[30] a) A. D. Becke, *J. Chem. Phys.* **1993**, *98*, 5648 – 5652; b) C. Lee, W. Yang, R. G. Parr, *Phys. Rev. B* **1988**, *37*, 785 – 789; c) P. J. Stephens, F. J. Devlin, C. F. Chabalowski, M. J. Frisch, *J. Phys. Chem.* **1994**, *98*, 11623 – 11627.

[31] A. K. Wilson, D. E. Woon, K. A. Peterson, T. H. Dunning, *J. Chem. Phys.* **1999**, *110*, 7667 – 7676.

[32] B. H. Besler, K. M. Merz, P. A. Kollman, *J. Comput. Chem.* **1990**, *11*, 431 – 439.

[33] N. L. Allinger, X. F. Zhou, J. Bergsma, *Theochem.* **1994**, *118*, 69 – 83.

[34] S. Bureekaew, S. Amirjalayer, M. Tafipolsky, C. Spickermann, T. Roy, R. Schmid, *Phys. Status Solidi B* **2013**, *250*, 1128 – 1141.

[35] W. Smith, T. Forester, *J. Molec. Graphics* **1996**, *14*, 136 – 141.

[36] J. M. Thijssen, Computational Physics (2nd ed.). Cambridge University Press **2007**, 226 – 231.